

## Risk perception for deep excavation based on results of numerical analysis

Hsiao-Chou Chao

Moh and Associates, Inc., 22FL. No.112, XinTai Wu Rd Sec 1, 22102, New Taipei City, Taiwan, R.O.C.

### ABSTRACT

Three-dimensional finite element method was applied to evaluate the design appropriateness and identify potential risks for a deep excavation project in close proximity to an MRT viaduct. The evaluation was performed independently without referring to the soil parameters and analysis method provided in the original design document. Geotechnical interpretation, numerical analysis, and functional requirements review were conducted in the study. Results of the evaluation show that the structural members or ground regions subject to the most significant influence can be identified straightforwardly in the three-dimensional domain and thus the risk precaution and hazard mitigation measure can be developed in a more precise manner.

**Keywords:** Three-Dimensional Finite Element Approach; Deep Excavation, Top-down Excavation Method; MRT Protection;

### 1 INTRODUCTION

In engineering practice, deep excavation and its influence on adjacent buildings or infrastructures are usually analyzed through one or two dimensional (1D or 2D) numerical approach with appropriate simplification or equivalence technique. Design or evaluation work is usually performed on selected cross-sections based on soil parameters interpreted from field and laboratory tests. Uncertainties arise from simplification made for geometries of complicate underground structures and assumptions for soils with high degree of variability are inevitable. It is not difficult to envision that engineers may lose sight of important perspectives for the soil-structural interaction behavior and thus result in inappropriate interpretation. With rapid development of the modern computer technology, the shortcomings can be improved by the three-dimensional (3D) numerical approach. More realistic perspective can be obtained and facilitate engineer to identify potential hazards in a more precise manner. A large-scale deep excavation project located in the proximity of a mass rapid transit viaduct is selected as a case study to demonstrate the application of the 3D numerical approach for engineering risk perception.

### 2 PROJECT DESCRIPTION

The project site of the case example is located on the eastern outskirts of Taipei Basin. Regional geology is composed of the Quaternary Alluvial and the underlying Miocene to Pliocene Kueichulim Rock Formation as shown in Fig.1.

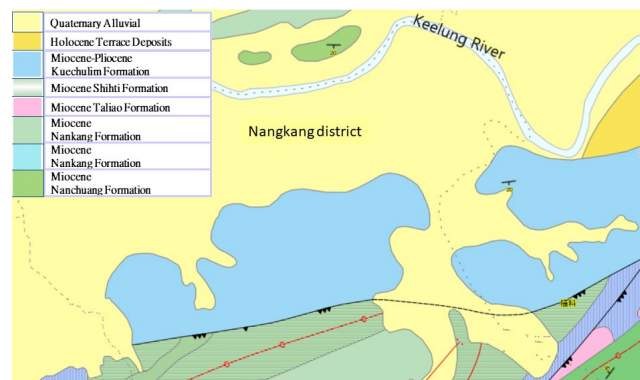


Fig. 1. Regional Geological Map (Central Geological Survey, MOEA, 2019)

The project comprises a complex structure with a central exhibition dome rises to the height of 60m enclosed by three tower buildings with the heights greater than 100m, altogether sit on top of a seven-story above ground podium. The five-story basement covers the footprint of about 30,000m<sup>2</sup> to the depth of 23m.

Protection of the MRT viaduct in the proximity area with the minimum clearance of 12m is critical for the success of the construction work. Excavation induced ground movement, and the tilt, lateral displacement, and differential settlement of the viaduct structure are evaluated carefully. Protection measures and monitoring scheme need to be specified with necessary construction control measures (MOTC, R.O.C., 2012).

### 3 EXCAVATION DESIGN

The integrated diaphragm-buttress wall was selected as the retaining structure for the excavation work. Parts of the plan layout is shown in Fig. 2. As a balance

strategy between construction cost and functional requirements such as providing sufficient structural stiffness for reducing the magnitude of structural deflection and restraining the ground movement to protect the MRT structures in the proximity area, accommodating the significantly varied top elevations of bedrock, and reducing the amount of groundwater inflow from outside zone during excavation, several types of diaphragm-buttress wall were proposed to form the retaining structure. Representative design features of the diaphragm-buttress wall are given in Table 1 and Table 2, respectively.

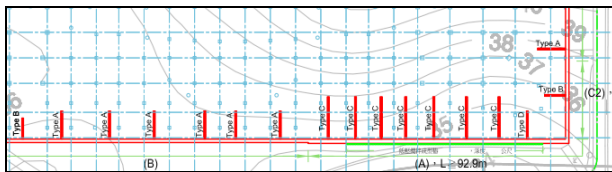


Fig. 2. Diaphragm-Buttress Wall Layout

Table 1 Design Summary for Diaphragm Wall (DW)

Type	Thickness (cm)	Depth (GL.-, m)	Control Criteria
A	150	≥36.0	At least 2.0m into the bed rock
B	120	≥36.0	
C2	120	≥36.5	At least 1.5m into the bed rock

Note: Reference elevation EL.11.22m;  $f'_c = 280 \text{ kgf/cm}^2$

Table 2. Design Summary for Buttress Wall (BW)

Type	Dimension (mm)	Depth (GL.-, m)	Concrete Strength $f'_c$ (kgf/cm <sup>2</sup> )
A	700×10,000	GL.-4.0~33.0	$f'_c = 175 \text{ kgf/cm}^2$
B	700×7,500	GL.-4.0~33.0	(above GL.- 16.3m);
C	700×15,000	GL.-2.0~35.0	$f'_c = 245 \text{ kgf/cm}^2$
D	700×10,000	GL.-2.0~35.0	(below GL.-16.3m)

Top-down excavation approach was selected as the construction method in which the floor slabs were treated as lateral supports. To expedite the excavation progress and provide sufficient space for construction activities and earth work, staged excavations are designed to proceed when the opening in the center of the immediate top slab above the excavation face is less than 33% of the total slab area. Proposed steps for excavation work are summarized in Table 3.

Table 3 Steps for Deep excavation and Basement Construction

Step	Excavation Depth (m)	Buttress Wall Above Excavation Face	Construction Activity Prior to Excavation
1	GL.-1.60	Demolish	Install DW and BW
2	GL.-7.12	Demolish	B1F w/ opening
3	GL.-11.62	Demolish	B1F closure; B2F w/ opening
4	GL.-15.02	Demolish	B2F closure; B3F w/ opening
5	GL.-18.42	Demolish	B3F closure; B4F (w/ opening
6	GL.-23.32	Retain	B4F closure; Raft
7		Demolish	B5F

Instrumentation and monitoring management scheme for protection of MRT viaduct is summarized

in Table 4 and illustrated in Fig. 3.

Table 4. Allowable Value for Monitoring Management

Item	Allowable Value
Diaphragm Wall	Deformation < 42mm (MRT Side)*
MRT Viaduct	Lateral Displacement < 15mm**; Tilt < 1/750** Differential Settlement < 1/1000** Ground Settlement < 55mm*

\* Design value;

\*\* MRT protection code (MOTC, R.O.C., 2012)

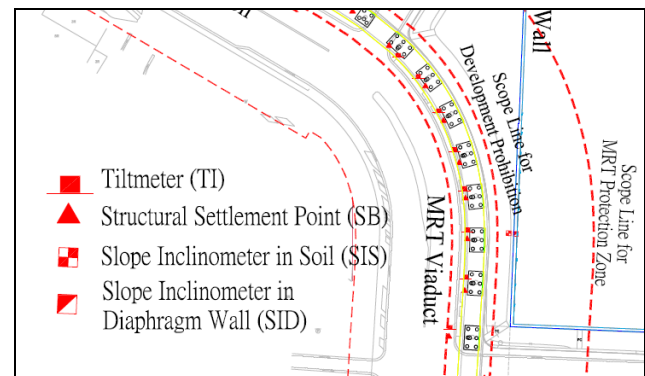


Fig. 3. MRT Viaduct Instrumentation and Monitoring Scheme (Taiwan Life, 2018b)

## 4 NUMERICAL EVALUATION

The 3D finite element approach was applied to check if the functional requirements for the proposed retaining system and MRT protection scheme can be satisfied. The analysis parameters and numerical model were developed based on the results of geotechnical investigation and geometry of design drawings without referring to the parameters and calculation methods used in the design document. The study followed the the procedure of geotechnical data interpretation, finite element analysis, and functional requirements evaluation. Results of the evaluation including geological profile, displacements of diaphragm wall, and movements of MRT viaduct foundations are presented below.

### 4.1 Geotechnical Interpretation

Geotechnical interpretation was conducted based on the field and laboratory test results derived from the twenty-six boreholes explored at the design stage.

The interpreted ground profile is illustrated by selected cross sections of borehole logs as shown in Fig. 4. As shown in the figure, the ground deposit of the site is composed of six interbedded silty sand and silty clay layers to a depth varied from 33m to 43m overlying on a gravel layer with maximum and mean thickness of 5.8m and 1.3m, respectively. The characteristic of the site deposits is consistent with that of the Songshan Formation of Taipei Basin. Based on the geotechnical investigation results, a bedrock composed of sandstone and shale stone to the end of drilling depth is underlaid by the gravel layer. Groundwater observation shows the

groundwater head at shallow depth and deep depth are at about GL.-3m (EL.+8m) and GL.-11m (EL.0m), respectively. The corresponding piezometric pressure profile is demonstrated in Fig. 5.

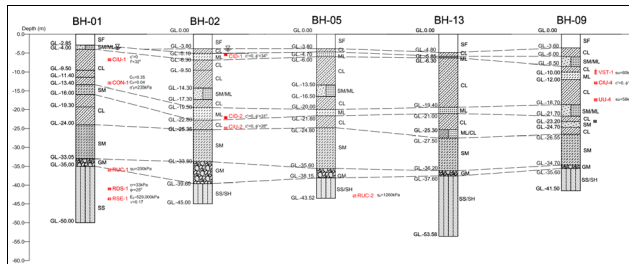


Fig. 4. Ground Composition Profile of BH-01, 02, 05, 13, and 09

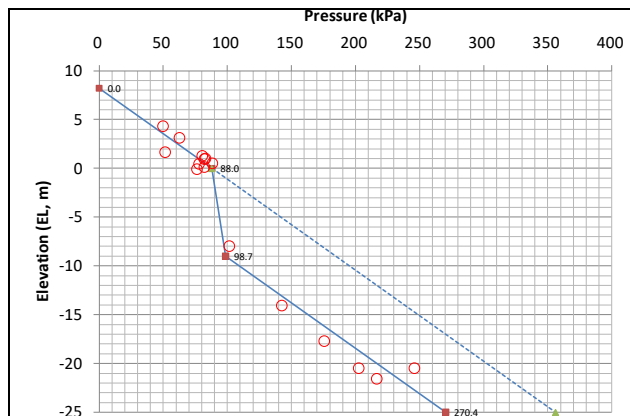


Fig. 5. Piezometric Pressure Profile of the Site

Soil classification, index properties and SPT-N values along the depth of ground of the site are illustrated by a borehole data shown in Fig. 6.

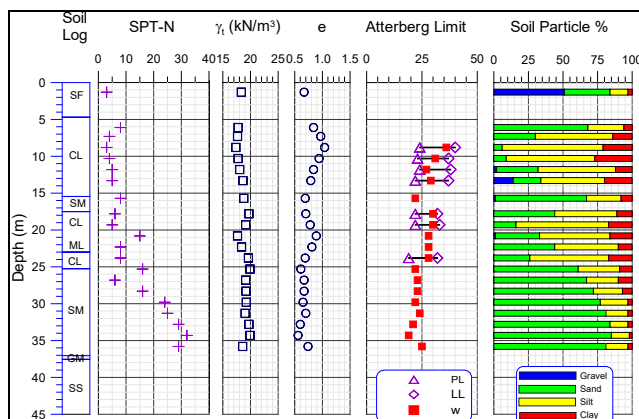
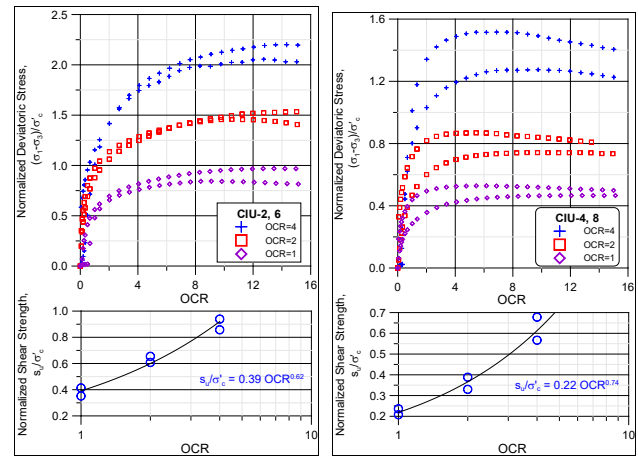


Fig. 6. Index Properties and SPT-N Values of BH-01

The undrained shear strengths  $s_u$  along the depth of clayey soils were estimated by the SHANSEP approach (Ladd and Foott, 1974) and is illustrated by Fig. 7. Correlations between the ratio of  $s_u$  to confining pressure  $\sigma'_c$  ( $s_u/\sigma'_c$ ) and overconsolidation ratio OCR are given in the lower portion of Fig. 7. The simplified soil properties and analysis parameters are listed in Table 5 and Table 6. Analysis parameters based on the results of triaxial consolidated drained tests (CID),

triaxial consolidated undrained tests (CIU), one dimensional oedometer tests (CON), and empirical correlations.



(a) Upper clay layer (b) Lower clay layer  
Fig. 7. Results of SHANSEP approach

Table 5. Simplified Soil Parameters

No	Soil Type	Depth (GL.-, m)	SPT-N	$\gamma_t$ (kN/m <sup>3</sup> )	$c'$ (kPa)	$\phi'$ (deg)	$s_u/\sigma'_c$ (kPa)
1	SF	2.3	8	19.0	0	31	-
2	CL	3.8	6	18.5	0	29	$0.39 \cdot OCR^{0.62}$
3	SM	5.9	4	18.3	0	29	-
4	CL	17.8	4	18.6	0	29	$0.23 \cdot OCR^{0.67}$
5	SM	20.0	14	18.6	0	31	-
6	CL	26.0	7	19.0	0	30	$0.22 \cdot OCR^{0.74}$
7	SM	33.0~43.0	21	18.9	0	33	-
8	GM	38.1	-	21.0	0	38	-
9	SS	-	-	21.9	0	38	-

Table 6. Analysis Parameters

Soil Layer	Bottom Depth (m)	$e$	OCR	$E_{50}^{ref}$ (kN/m <sup>2</sup> )	$E_{oed}^{ref}$ (kN/m <sup>2</sup> )	$E_{ur}^{ref}$ (kN/m <sup>2</sup> )	Drainage Type
SF	2.3	0.70	-	-	-	-	Drained
CL-1	3.8	0.83	4.0	7,100	4,740	21,310	Undrained
SM-1	5.9	0.82	-	7,920	7,920	23,760	Drained
CL-2	17.8	0.84	1.1	7,770	5,180	23,310	Undrained
SM-2	20.0	0.75	-	14,470	14,470	43,410	Drained
CL-3	26.0	0.76	1.0	8,840	5,890	26,510	Undrained
SM-3	33.0~43.0	0.70	-	12,630	12,630	37,900	Drained

Note: for use in the Hardening Soil Model

## 4.2 Numerical Calculation

Behaviors of site soils and underlying gravel and bedrock were simulated by the Hardening Soil Model and the Mohr Coulomb Model, respectively. The geometrical model built in the Plaxis 3D (Plaxis b.v. 2018) is shown in Fig. 8. The finite element mesh generated thereafter for numerical simulation is composed of 256,868 elements. The soil-structural interaction as a result of excavation was simulated with the construction steps in Table 4. Groundwater head was kept at 1m below the excavation face with the excavation. Calculated maximum and corresponding control criteria are summarized in Table 9.



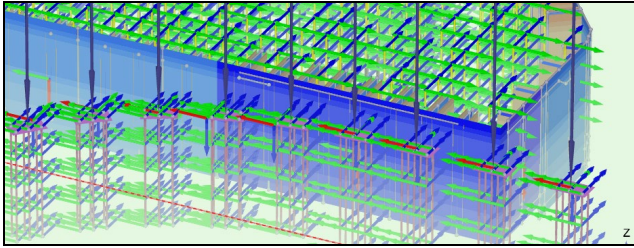


Fig. 8. Geometric model built in Plaxis 3D

Table 9. Summary of evaluation results

Item		Computed Maximum	Allowable Value
Ground settlement		45mm	55mm
DW Displacement	MRT Side	42mm	42mm
MRT Viaduct	Lateral Displacement	15mm	15mm
	Tilt	0.17/750	1/750
	Differential Settlement	0.12/1000	1/1000

Computed maximum surface settlement contour is shown in Fig. 9 in which the maximum value between the MRT viaduct and excavation site are observed to have the magnitude of 30mm. The maximum lateral displacement of the diaphragm wall observed at MRT side is 41mm as shown in Fig. 10. For the MRT viaduct, the maximum lateral displacement is observed to occur with the magnitude 15mm at P1007 and P1008 as shown in Fig. 10 and Fig. 11. The maximum tilt is observed to occur at P1009 with the magnitude of 0.17/750 while the maximum differential settlement is observed to occur between P1008 and P1009 with the magnitude of 0.12/1000.

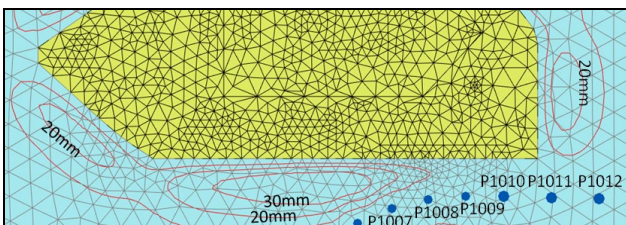


Fig.9. Contour of Maximum Surface Settlement

Results of the numerical evaluation show that the reactions of the MRT viaduct and retaining system including lateral displacement, tilt and differential settlement to the deep excavation work are comply with the MRT protection requirements.

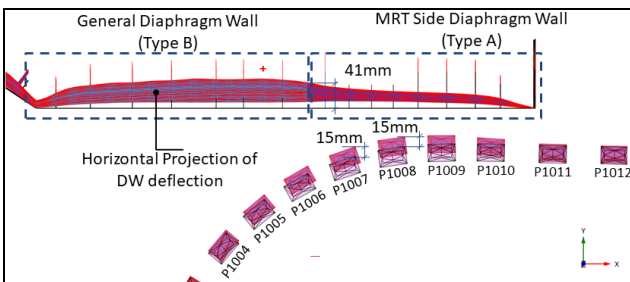


Fig.10. Superimposed Horizontal Projections of the Lateral Displacement of the Diaphragm Wall and MRT Pile Caps

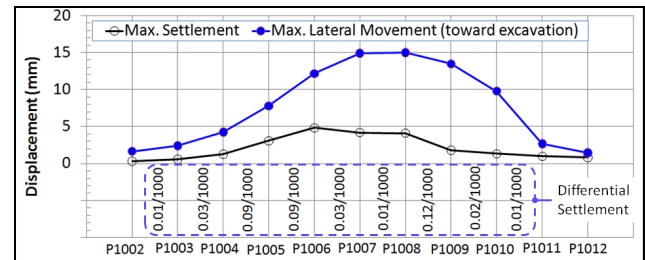


Fig.11. Computed MRT Viaduct Displacement and Settlement

## 4 CONCLUSION

The 3D finite element approach allows engineer to stratify the region in a 3D space in which the maximum displacement or stress could occur. This approach eliminates the need in 1D or 2D design approach to determine the most critical cross sections by personal judgment before analysis and thus avoid dealing with the associated uncertainties.

For the demonstrated case example, the computed maximum lateral displacement is virtually equal to the allowable limit and thus the likelihood of the actual performance exceeding the allowable limit can not be neglected. To mitigate the risks resulted from adverse factors such as poor construction control or variability of ground properties, ground improvement before start of excavation, cautious construction control measure, careful instrumentation and monitoring scheme, and emergency response plan should be developed and incorporated into the design conclusion.

## ACKNOWLEDGEMENTS

The authors are grateful to Dr. Za-Chih Moh for his support during the preparation of this paper.

## REFERENCES

- Plaxis b.v. (2018). Plaxis 3D Reference Manual.
- Central Geological Survey, MOEA, R.O.C. (2019). Integrated Geology Database, <http://gis.moeacgs.gov.tw>
- Ladd, C.C. and Foott, R. (1974). A New Design Procedure for Stability for Soft Clays," Journal of the Geotechnical Engineering Division, ASCE, Vol.100, No. GT7, pp763-786.
- MOTC, R.O.C. (2012). Regulations for Prohibition and Restriction on Development in the Proximity Area of Mass Rapid Transit System.